Annealing effects on phase transformation and optical enhancement of $CuInSe_2$ film solar cells

XIN JI [*], JUN CHEN DENG [a], JIAN YONG TENG[**], ZHI YAN[b], YI MING MI, CHAO MIN ZHANG
College of Fundamental Studies, Shanghai University of Engineering Science, Shanghai 201620, China
[a]*College of Urban* Railway *Transportationg, Shanghai University of Engineering Science, Shanghai 201620, China*
[b]*College of Material Engineering, Shanghai University of Engineering Science, Shanghai 201620, China*

Sputtering deposited $CuInSe_2$ films are of potential important as absorber material in thin-film solar cells as long as we can optimize the annealing process to enhance their optical properties. The aim of the present study is to find the phase transformation mechanism and predict the enhanced optical behaviour of $CuInSe_2$ films as a result of annealing processes. The results show that low-temperature annealing processes not exceeding 250 °C can produce regrown and recrystallised $CuInSe_2$ phases to enhance the conversion efficiency of $CuInSe_2$ solar cells. High-temperature annealing processes (at 350 and 400 °C) are found to be vital for the transformation from the $CuInSe_2$ phase to $CuSe_2/Cu_{2-x}Se$ and $InSex/In_2Se_3$ structures. Finally, three selenization models related to the selenisation of the annealing processes are proposed.

(Received July 9, 2013; accepted November 7, 2013)

Keywords: $CuInSe_2$ film, Annealing processes, Phase transitions, Vapor deposition, Optical properties

The sputtering method is the most popular metal transformation process for producing complex alloys [1, 2], since it is capable of producing different components, and also because of its great economic advantages and high production rates.

Primarily in the energy industry, this method is very important for control of the composition of solar cell device materials [3-5]. $CuInSe_2$ (CIS) films or other promising solar cell materials can be produced, with pure structures. Annealing is one of the most efficient and cost-effective methods for producing accurate composition and for achieving phase transformations during the sputtering stage.

The annealing process is becoming very important because of the increase in the manufacturing of electric parts between conductive and absorbing layers [6, 7]. Annealing processes can have a purely protective function [8, 9], or be used for improving the optical properties of solar cell films [10], and they are also able to hide superficial defects or modify surface properties. A manufacturer's objective is to produce these types of parts whilst minimising costs [11]. This can be achieved by minimising the production time of each layer, i.e. by reducing the insulated parts in the deposition cycle [12]. If this superficial aspect can be addressed during the annealing process, then production time and material needs can be reduced.

Over the last few years, various authors have studied the annealing process used for energy materials [13, 14]. The main aspect studied has been the effect of the annealing process on synthesis and surface characteristics during the deposition cycle; however, this directly affects the structural changes when one layer is linked to another. None of the previous reports mentions this latter aspect, and no one considers the possibility of improving the optical properties. There are no references to these kinds of studies when the films are used in solar cells. In this article, an annealing process is designed to speed up the phase transformation of CIS films, in order to find a useful method for the manufacture of highly effective CIS film solar cells. Also, three selenization models are proposed to optimise the electrical and optical properties of CIS layers before manufacturing series of parts.

1. Experiment

1.1 Synthesis of CIS thin films

Solar cells were fabricated with the structure SFO/CdS/CIS. A CdS buffer layer was deposited first on an SFO (SnO_2: F) glass using 50 W power, and then the CIS adsorbed layer was deposited at 100 W power on the CdS window layer. Thin films of CIS and CdS were all deposited by radiofrequency sputtering using a magnetron sputtering system (FJL560D2). Cylindrical $CuInSe_2$ (Cu:In:Se = 1:1:2) and CdS ceramic targets of 8 cm in diameter were used. No changes in target composition were observed with time and usage. The deposition chamber's base pressure was 1.6×10^{-4} Pa, and during deposition, the gas pressures were maintained constant at 0.5 Pa. The substrate-to-target distance was 100 mm. Depositions of CIS and CdS layers were performed at room temperature for 180 and 25 min, respectively. Finally, the layers of CIS/CdS were heat treated in a vacuum with annealing

processes at different temperatures (200, 250, 350 and 400 °C) for 60 min.

1.2 Characterizations of CIS films

Optical properties of the CIS layers were measured at normal incidence using a double-beam ultraviolet–visible–near-infrared spectrophotometer (Shimadzu) with optical transmittance in the photon energy range of (1.76–10.56) × 10^{-19} J. To investigate the crystallographic properties of the films, coupled θ–2θ X-ray diffraction (XRD) scans were performed in the range 2θ = 20–80° by use of the Cu $K_{\alpha 1}$ line of an X-ray source (Rigaku D/max2550). The surface morphologies of films were examined by atomic force microscopy (DI Nanoscope IIIA Multimode), and the cross-sectional morphologies were examined by scanning electron microscopy (SEM-3400-N).

2. Results and discussion

2.1 Effects of annealing processes on phase trans formation

Fig. 1 shows the XRD patterns of CIS films prepared at various annealing processes. For the as-deposited film, the formation of minor chalcopyrite phase-like CIS (1 1 2), (2 2 0) and (2 1 1) planes and tetragonal phase-like CIS (3 1 0), (3 1 2) and (4 0 0) planes was observed [15]. In the case of films annealed at 200 and 250 °C, the preferential orientation of the planes in the films became much stronger, which indicated that CIS particles of better crystallinity and larger grain size were formed during low-temperature annealing processes not exceeding 250 °C. Obviously, the annealing process contributes to the diffusion of atoms adsorbed on the substrate and accelerates the migration of atoms to energetically favourable positions, resulting in an enhancement of the crystallinity [16]. With an increase in annealing temperature to 350 °C, two small XRD peaks are observed around 33° and 62°, which indicate the existence of $CuSe_2$ and $InSe_x$ structures. This transformation from CIS phase to $CuSe_2$ and $InSe_x$ structures is associated with the evaporation of indium and selenium in the intermediate-temperature annealing process. When the annealing temperature was increased further to 400 °C, the $CuSe_2$ and $InSe_x$ peaks disappeared completely, and strong $Cu_{2-x}Se$ and In_2Se_3 peaks appeared. This behaviour implied that the transformation from CIS to $Cu_{2-x}Se$ and In_2Se_3 required a high-temperature annealing process owing to the slower diffusion kinetics. It is clear that low-temperature annealing processes not exceeding 250 °C can produce a highly effective CIS solar cell that contains the single CIS phase in the CIS absorbing layer.

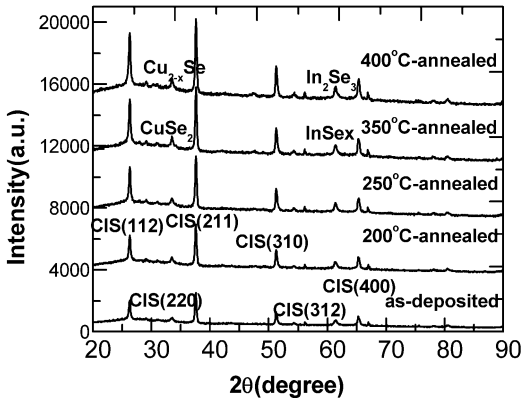

Fig. 1. XRD patterns of $CuInSe_2$ films prepared at various annealing temperatures.

2.2 Effects of annealing processes on grain growth

Fig. 2(a)–(e) shows the atomic force microscopy surface morphologies of as-deposited CIS films and CIS films annealed at temperatures of 200, 250, 350 and 400 °C, respectively. It is found that the annealing process has a great influence on grain nucleation and growth. The as-grown CIS layer contained a high density of vacancy defects, which led to a large surface roughness, as indicated in Fig. 2(a). In addition, it can be seen in Fig. 2(b), (c) that the CIS grains in the films annealed at 200 and 250 °C seem to be rather compact and dense. Obviously, low-temperature annealing processes can improve the surface diffusion and cause the grains to regrow and recrystallise. Furthermore, as shown in Fig. 2(d), (e), the films annealed at 350 and 400 °C exhibited a columnar structure and the surfaces became rougher, which shows that it is easy for the grains to agglomerate with each other through a thermally activated growth mechanism during annealing at the highest temperatures. In addition, it was found that increasing the annealing temperatures increased the lattice mismatch and decreased the mobility of holes in the films.

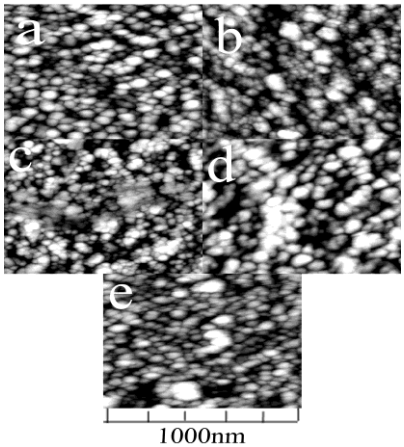

Fig. 2. AFM images of $CuInSe_2$ films prepared at various annealing temperatures: (a) As-deposited; (b) 200°C; (c) 250°C; (d) 350°C; (e) 400°C.

The cross-sectional morphologies of the CIS films annealed at different temperatures are shown in Fig. 3. It can be seen from Fig. 3(a), (b) that the CIS film annealed at 200 °C had a much thicker section than the as-deposited film, which confirms the occurrence of regrowth and recrystallisation as indicated by the XRD patterns. It can be seen in Fig. 3(c) that the density of grains was increased with increasing grain sizes at the CIS/CdS interface, which was considered to be because of the reconstruction and improvement in the CIS crystals at the supplement of high energy for the annealing process at 250 °C. For the films annealed at 350 and 400 °C (Fig. 3(d), (e)), it is seen that the interface is destroyed, with some cracks between the grains being present in the films, which implies that phase transformation occurs accompanied by evaporation of indium and selenium.

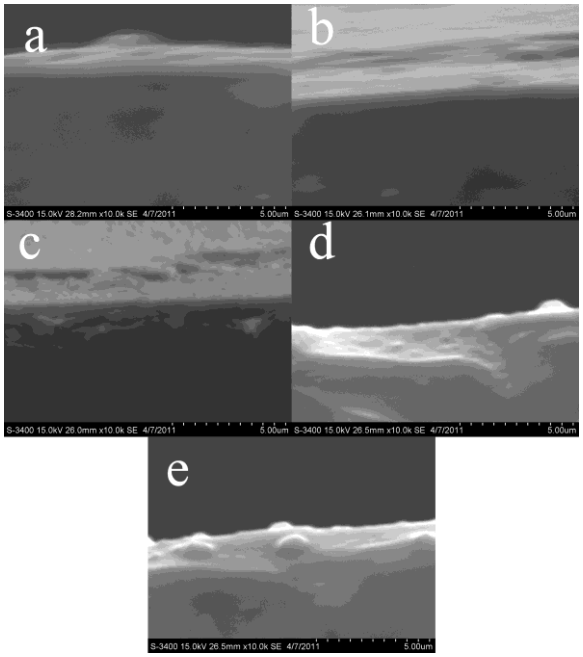

Fig. 3. SEM cross-section morphologies of CuInSe2 films prepared at various annealing temperatures: (a) As-deposited, (b) 200°C, (c) 250°C, (d) 350°C, (e) 400°C.

2.3 Effects of annealing processes on optical properties

Fig. 4 shows the absorption spectra of $CuInSe_2$ films deposited with different annealing temperatures. It clearly shows an improvement in the optical performance f the CIS film after annealing at 250 °C compared to that of the other annealed temperatures.

Experimental values of $(\alpha h\nu)^2$ against $h\nu$ for the CIS/CdS layers are plotted in Fig. 5. The optical band gap E_g can be determined with the help of the following relation [17]:

$$\alpha = A/h\upsilon(h\upsilon - E_g)^{1/2} \quad (1)$$

where A is a constant and $h\nu$ is the radiation energy. Fig.5 shows that the optical band gap E_g of CIS/CdS layers varies from 3.55×10^{-19} to 3.73×10^{-19} J, with the annealing temperature varying from 250 to 400 °C.

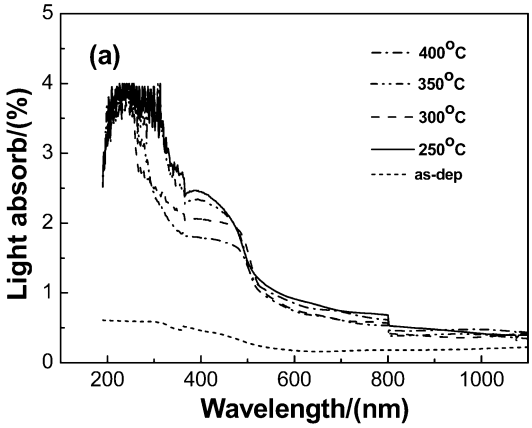

Fig. 4. Absorption spectra of $CuInSe_2$ films deposited with different annealing temperatures.

It can be seen in Fig. 5 that the band gaps of the CIS films increased initially, and then decreased with increasing annealing temperature. Evidently, the low-temperature annealing processes not exceeding 250 °C cause a significant increase in the optical band gap close to the best absorbed band gap of sunlight. In addition, it can also be observed that the high-temperature annealing processes at 350 and 400 °C can destroy the CIS/CdS conductive layer with a high density of vacancy defects, which leads to a loss of positron trapping at these increased numbers of vacancies. Therefore, controlling the optical band gap using the low-temperature annealing processes is a good way to enhance the conversion efficiency of a CIS solar cell.

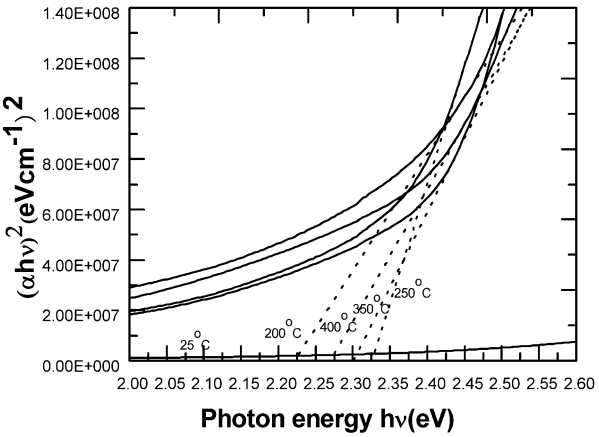

Fig. 5. Plot of $(h\upsilon)^2$ versus $h\upsilon$ for the $CuInSe_2$ films prepared at various annealing temperatures.

2.4 Possible selenisation models for the annealing processes

It was reported by Milton [18] that the selenization mechanism of three-element alloy films (Se particles adsorbed to Cu and In particles) can be represented through three models: slow selenization model, rapid selenization model and non-selenization model. Therefore, three models for the sputtering process are proposed (Fig. 6). For the first model (slow selenization model), applicable for films annealed at 25 °C with lower surface energy, the selenization reaction by Se, Cu and In particles takes place, and as a consequence, two phases appear in the films. For the second model (rapid selenization model), induced at 200 and 250 °C with higher surface energy, the formation of the more stable CIS phases occurs. Finally, for the third model (non-selenization model), induced at 350 and 400 °C with the highest surface energy, when the sputtering temperature reaches the evaporation temperature of indium and selenium, formation of $Cu_{2-x}Se$ and In_2Se_3 structures in the CIS films occurs.

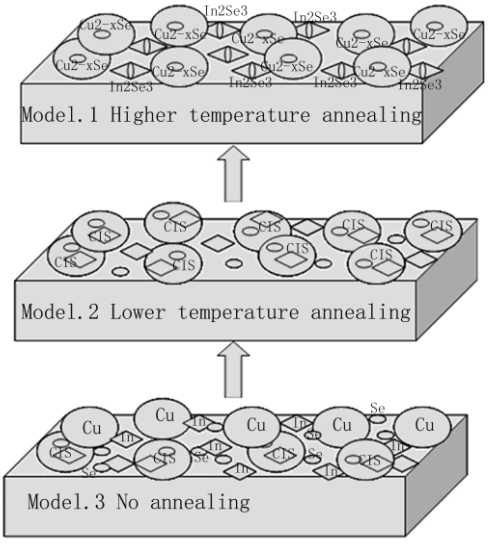

Fig. 6. Selenization models of $CuInSe_2$ films deposited at various annealing temperatures.

3. Conclusions

In conclusion, we systematically investigated the phase transformation and optical properties of $CuInSe_2$ films with different annealing processes. This indicates that low-temperature annealing processes not exceeding 250 °C can produce pure chalcopyrite and tetragonal CIS phases. In addition, high-temperature annealing processes have a strong effect on the transformation from the CIS phase to $CuSe_2/Cu_{2-x}Se$ and $InSe_x/In_2Se_3$ structures. We find that low-temperature annealing processes not exceeding 250 °C could cause a significant increase in the optical band gap, which can be used to enhance the conversion efficiency of CIS solar cells. Finally, we proposed three models to explain the relationship between the selenisation and annealing processes.

Acknowledgements

This work is supported by the Shanghai Municipal Education Commission's Funds for the Outstanding Young Teachers in High Education Institution (No: shgcjs021), the College Innovation Program of the Shanghai Municipal Education Commission (No: cs1321007) and the Science and Technology development Fund of Shanghai University of Engineering Science (No: 2012gp41).

References

[1] X. Ji, Z. Yan, Y. M. Mi, C. M. Zhang, Optoelectron. Adv. Mater. – Rapid Comm. **6**(3-4), 483 (2012).
[2] X. Ji, Z. Yan, Y. M. Mi, C. M. Zhang, Optoelectron. Adv. Mater. – Rapid Comm. **6**(1-2), 300 (2012).
[3] M. A. Popescu, J. Non-Cryst. Solids. **169**(1-2), 155 (1994).
[4] M. A. Popescu, J. Non-Cryst. Solids. **35-36**, 549 (1980).
[5] I. Miron, I. Grozescu, Optoelectron. Adv. Mater. – Rapid Comm. **6**(5-6), 637 (2012).
[6] U. Alver, A. Kudret, S. Kerli, Optoelectron. Adv. Mater. – Rapid Comm. **6**(1-2), 107 (2012)
[7] N. Touka, B. Boudine, O. Halimi, M. Sebais, Optoelectron. Adv. Mater. – Rapid Comm. **6**(5-6), 583 (2012).
[8] V. Mdgil, V. S. Rangra, Optoelectron. Adv. Mater. Rapid Comm. **7**(1-2), 30 (2013).
[9] B. B. Nariya, A. K. Dasadia, A. R. Jani, Optoelectron. Adv. Mater. -Rapid Comm. **7**(1-2), 53 (2013).
[10] A. K. Dasadia, B. B. Nariya, A. R. Jani, Optoelectron. Adv. Mater. – Rapid Comm. **7**(1-2), 70 (2013).
[11] A. Sathiya Priya, I. B. Shameem Banu, J. Thirumalai, A. Alagar, Adv. Mater.–Rapid Comm. **7**(3-4), 191 (2013).
[12] I. N. Askerzade, R. T. Tagiyeva, N. Guclu, Optoelectron. Adv. Mater.–Rapid Comm. **7**(3-4), 276 (2013).
[13] D. E. Baciu, J. Simitzis, Optoelectron. Adv. Mater. – Rapid Comm. **7**(3-4), 296 (2013).
[14] M. Bacalum, B. Zorila, M. Radu, A. Popescu, Optoelectron. Adv. Mater. – Rapid Comm. **7**(5-6), 456 (2013).
[15] Z. Li, H. Qing, W.L. Jiang, F.F. Liu, C.J. Liu, S. Yun, Sol. Energy Mater. Sol. Cells. **93**, 114 (2009).
[16] M. Venkatachalam, M.D. Kannan, S. Jayakumar, R. Balasundaraprabhu, N. Muthukumarasamy, Thin Solid Films **516**, 6848 (2008).
[17] K.C. Sharma, R.P. Sharma, J.C. Garg, J. Phys. D: Appl. Phys. **25**, 1019 (1992).
[18] O. Milton, Materials science of thin films, Second ed., Academic Press, New York, 2006.

*Corresponding author: jixin@sues.edu.cn
**jyteng@sues.edu.cn